Original Paper

In-depth analysis of elements and properties of hydrated subsurface layers on optical surfaces of a SiO_2–BaO–B_2O_3 glass with SIMS, IBSCA, RBS and NRA

Part 1. Experimental procedures and results

Hans Bach
Schott Glaswerke, Mainz (FRG)

Klaus Großkopf
Carl Zeiss, Oberkochen (FRG)

Peter March and Friedrich Rauch
Institut für Kernphysik der Johann-Wolfgang-Goethe-Universität, Frankfurt am Main (FRG)

The formation of thin subsurface layers was studied which occurred during the chemical interaction of polished and cleaned optical surfaces with different slurries before and after covering them with $\lambda/4$-MgF_2 coatings. By a suitable selection of the parameters for these chemical interactions a thickness of the subsurface layers was produced which allowed to meet the requirements of the various surface analysis methods. The thicknesses and the refractive indices of the subsurface layers could be calculated from the measured spectral reflectances. Slurries with a pH value < 9 were applied so that a leaching of glass components from the subsurface layers occurred. This was indicated by the refractive indices and was studied in detail by analyzing the in-depth distributions of the glass components. Distinct matrix effects could be disclosed from the in-depth profiles for SIMS and IBSCA by a comparison with the results of the quantitative analysis with RBS and NRA. These matrix effects were different within the subsurface layers from those observed for the bulk glass. The quantitative analysis of the hydrogen in-depth distributions by NRA allows for the first time to link differences in the matrix effects with a different hydrogen content within the subsurface layers.

Untersuchung der Element-Tiefenverteilungen und Eigenschaften hydratisierter Oberflächenschichten auf optischen Flächen eines SiO_2–BaO–B_2O_3-Glases mit SIMS, IBSCA, RBS und NRA

Teil 1. Experimentelle Grundlagen und Ergebnisse

Es wurden Oberflächenschichten vor und nach Belegen mit $\lambda/4$-MgF_2-Schichten untersucht, die durch chemische Wechselwirkung mit verschiedenen Polierbrühen auf polierten und gereinigten optischen Flächen gebildet worden waren. Die für die verschiedenen Oberflächenanalysenmethoden erforderlichen Schichtdicken wurden durch geeignete Wahl der Parameter für diese chemische Wechselwirkung eingestellt. Die Schichtdicken und die Brechungsindizes der Oberflächenschichten wurden aus der jeweils gemessenen spektralen Reflexion errechnet. Durch Verwendung von Polierbrühen mit pH-Werten < 9 wurden Glaskomponenten aus der Oberfläche ausgelaugt. Dies wurde durch die Brechungsindizes angezeigt und durch Analyse der Tiefenverteilungen der Glaskomponenten im einzelnen untersucht. Aus dem Vergleich von SIMS- und IBSCA-Tiefenprofilen mit quantitativen RBS- und NRA-Analysen konnten deutliche Matrixeffekte ermittelt werden. Diese Matrixeffekte für die Oberflächenschichten waren von denen des kompakten Glases verschieden. Die quantitative Analyse der Wasserstoff-Tiefenverteilungen gestattete es erstmals zu zeigen, daß die Unterschiede in den Matrixeffekten mit verschiedenen Wasserstoffkonzentrationen in den Oberflächenschichten verknüpft sind.

1. Introduction

Thin subsurface layers develop during polishing on optical surfaces by the interaction with the aqueous solution of the polishing slurry. Their thickness depends on the parameters applied during polishing (see [1 to 4] and the literature cited in these contributions). The physical and chemical properties of such layers are different from those of the bulk glass [5 to 13]. Especially their mean refractive index mostly is smaller than that of the bulk and therefore the optical properties of the surfaces will be influenced by these thin subsurface layers [1 to 4]; [6 to 11]. The colour changes produced by compositional inhomogeneities of the subsurface layers are well-known in the optical fabrication as "staining". Obviously these inhomogeneities and variations of the thickness should be avoided in fabrication. Also a high degree of reproducibility of the optical surfaces on glass will be required. Therefore, it is important to investigate whether the attack of the slurry can be understood from what is known about the composition changes during the interaction of the glass surfaces with aqueous solutions. Furthermore, it will be necessary to find out whether detectable composition changes can be induced when parameters of the polishing process and other subsequent processes during cleaning are changed and how far these changes are linked with a change of the optical properties, e. g. [1 to 4 and 6 to 10].

Based on this knowledge, measures can be taken to provide a sufficient reproducibility of the optical surfaces and to avoid staining.

Received 2 February 1986, revised manuscript 10 July 1986.

The purpose of this contribution was twofold. First it was intended to show that the surface analysis methods SIMS, IBSCA, RBS and NRA[1]) can complement each other to provide a better understanding of the results of the in-depth analysis within the subsurface layers of the glass obtained with the different methods. The second aim was to obtain further information on the interaction of the slurry with the glass surface which will be important for meeting the requirements of the optical fabrication process. Results will be given of the in-depth analysis of subsurface layers developed on the optical surfaces of the barium- and boron-containing silicate glass SK 16, which were produced by interaction with the polishing slurry of a constant pH value and duration and different thermal treatments before and after coating with $\lambda/4$-MgF_2 layers. The relevance of these results for the optical fabrication was derived from a comparison with the spectral reflectance of the respective coated and uncoated optical surfaces on SK 16 glass in the range between $\lambda = 375$ nm and $\lambda = 775$ nm. This comparison was expected to contribute also to the knowledge of chemical and physical processes occuring between the aqueous solutions and oxide glasses.

2. Experimental

2.1. Selection of the analysis methods

Secondary ion mass spectrometry (SIMS) is well-suited to study the processes connected with leaching of a glass surface because its detection sensitivity is rather high for all elements [14]. It is advantageous to apply SIMS in combination with spectrochemical analysis (IBSCA) [15 and 16]. In the present investigations, characteristic differences between the radiation intensities of the emission lines of the excited sputtered neutral atoms and secondary ions were observed. For a comparison of the applicability of different analysis methods on glass surfaces and surface layers, see [14]. An in-depth resolution of a few nanometers can be obtained with both methods

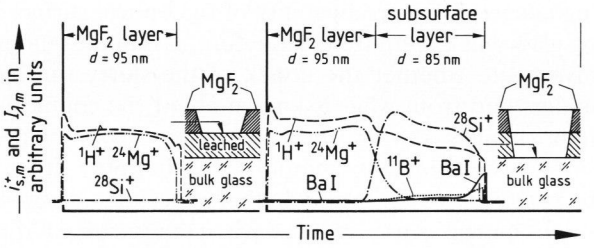

Figure 1. In-depth calibration and in-depth profiling: The in-depth ion-beam milling was stopped at the respective interfaces. The in-depth calibration can be obtained from the measurement of the etch pit depths using the shift of interference fringes.

[1]) SIMS = Secondary Ion Mass Spectrometry; IBSCA = Ion Beam Spectro-Chemical Analyzer; RBS = Rutherford Backscattering Spectrometry; NRA = Nuclear Reaction Analysis.

for material which can be sputtered homogeneously, see [4, 17 to 21] and in particular the descriptions for a variety of methods given in [17].

For the present investigations the quadrupole mass spectrometer and the monochromator of the BALZERS IEU 100 equipment (BALZERS AG, Liechtenstein) was applied for the investigations of the in-depth distributions of the components within the coatings and the subsurface layers.

During the ion-beam etching, etch pits were developed with well-defined bottoms parallel to the former surface [15]. The time dependence of the profiles could be converted into a depth dependence with a sufficiently good accuracy by measuring the depths d of the etch pits with interferometry; for further details on the equipment, see [4, 14 and 15]. Especially the thicknesses d of the coating and of the subsurface layers developed during leaching were determined in this way. For this purpose the ion-beam etching was interrupted when the interface between the coating and the glass surface or that between the subsurface layer and the bulk glass were reached. The positions of these interfaces were taken as the steepest slopes of the S-like changes observed for the recorded secondary ion currents of those components whose concentration was changing (figure 1). The letter d denotes in the following any depths below the surface determined in this way, or any thickness of the hydrated subsurface layers or of the coatings.

It is well-known that steep concentration gradients or concentration steps will be transformed into such S-like changes. This transformation is due to a number of disintegration phenomena which are linked with the ion-sputtering processes, e.g. [14, 17 and 18] and the literature cited in [19] considering insulating material.

For the discussion of the results it must be remembered that the secondary ion current $i_{s,m}$ or the intensity of the excited radiation $I_{\lambda,m}$ of the element m can be related with the concentration C_m by the equations (1 and 2) [20 and 21]:

$$i^{\pm}_{s,m} = i_p \cdot S \cdot C_m \cdot p^{\pm}_m \cdot K_m ; \quad (1)$$

$$I_{\lambda,m} = i_p \cdot S \cdot C_m \cdot \alpha_{\lambda,m} \cdot K_{\lambda,s} \quad (2)$$

with i_p the primary ion current, S the total sputter yield (number of sputtered atoms/number of impinging projectiles), $p^{\pm}_m$ the ionization coefficient for the element m, $\alpha_{\lambda,m}$ the excitation coefficient for the spectral line with the wavelength λ of the element m, K_m the factor which accounts for the detection sensitivity of the mass spectrometer, $K_{\lambda,s}$ the factor which accounts for the geometry and the detection sensitivity of the spectrograph for this wavelength.

The quantities $p^{\pm}_m$ and $\alpha_{\lambda,m}$ and thus the detection sensitivities generally depend on the composition of

the material. Therefore the recorded secondary ion currents $i_{s,m}$ and the intensities of the spectral lines $I_{\lambda,m}$ are in general not proportional to the concentrations C_m but depend on the composition of the material [22 and 23]. This phenomenon is called "matrix effect". This has to be considered for the interpretation of the results.

On the other hand it has been shown that the in-depth distributions of cations can be analyzed quantitatively with a negligible error by IBSCA from a comparison of the IBSCA in-depth profiles with the electrochemical properties of the surface of oxide glasses [19]. A matrix effect was not observed for oxide minerals either [21]. Therefore, for the SK 16 glass and its subsurface layers considered here, it was expected that a quantitative analysis of the main glass components within the subsurface layers would be possible.

Surface potentials can disturb the in-depth distributions of cations. Therefore, a low-energy electron source was used for the discharge of the surface during SIMS and IBSCA analysis. The current densities of the mostly applied 150 eV electrons were chosen so that the time-dependent changes of the $^1H^+$ secondary ion currents were minimized which are characteristic for surface-potential-induced drift, see [24]. These electron beam densities were about 10 $\mu A/cm^2$. A better discharging was obtained when a Ta diaphragm was applied at the same time, see also [25]. An influence of the surface potentials on the aperture of the quadrupole mass spectrometer was not observed in the experiments presented here.

It is well-known from earlier work [6 to 8] and more recent investigations [10, 26 to 31] that water can be introduced into a subsurface layer of silicate glasses during an interaction of the glass surface with aqueous solutions by an exchange of hydronium ions [30] or molecular water [29] against the cations of the glass. This introduction of water can also influence the kinetics of chemical reactions which can occur during processes after polishing and cleaning and which can be essential for the optical properties of the surfaces [4]. Therefore, a quantitative analysis of the hydrogen in-depth distribution was required. A quantitative analysis with SIMS or IBSCA can only be made using calibration standards of known composition, see [20 and 21]. However, standards are not available for the thin subsurface layers considered here. The in-depth distribution of water cannot be disclosed also from the in-depth distributions of oxygen on the surface of glasses. This is different from the investigations on metal surfaces in which case the spectroscopy of photon-induced secondary electrons can be applied. Therefore, as a third method nuclear reaction analysis (NRA) was employed for the investigation of the subsurface layer formation.

This method has been applied successfully for studies on the introduction of water into subsurface layers of other silicate glasses [26, 27 and 30]. NRA has a sufficient detection sensitivity for hydrogen and shows no matrix effect so that the calibration can be done with a variety of other compounds which contain hydrogen. Furthermore, the in-depth resolution of better than 10 nm is sufficient for subsurface layers of the thickness considered here.

Additional measurements were performed using RBS, which yields quantitative information on the heavier glass constituents, barium and silicon in the present case.

The NRA method used for analyzing hydrogen is based on the resonance reaction

$$^1H + {}^{15}N \rightarrow {}^{12}C + {}^4He + 4.43\ \text{MeV}\ \gamma\ \text{radiation}.$$

Since this method has been discussed previously in detail [26 and 27], it will be described here only briefly. The 4.43 MeV γ rays emitted from the sample are measured with a NaI scintillation detector; their number is proportional to the local hydrogen concentration. By raising the ^{15}N energy from the resonance energy, $E_{res} = 6.40$ MeV, stepwise to higher values and measuring at each energy the number of γ rays, the hydrogen concentration at increasing depth in the sample can be determined. The in-depth resolution is about 8 nm at the sample surface and decreases slowly with increasing depth; e. g., at 400 nm depth it is about 30 nm. Absolute hydrogen concentration values can be obtained with an uncertainty of about 10 %. This uncertainty is mainly due to the uncertainties of the energy-loss values for ^{15}N ions [32] which enter into the analysis of the measuring data.

The RBS method and its application for the analysis of materials is described in detail elsewhere [33]. In short, the sample is bombarded with a beam of energetic ions (^4He ions of 2.8 MeV in the measurements). These ions can be elastically scattered in the Coulomb field of atomic nuclei. In such a collision, whose cross section is well-known (Rutherford cross section), a large amount of energy is transferred to the target nucleus, so that the direction of the projectile may be changed significantly. Projectiles scattered at backward angles can leave the sample and their energy can be measured with a suitable detector. Since the energy after scattering depends on the mass of the scattering partner, one obtains information on the composition of the sample. By taking into account the continuous electronic energy loss of the projectiles before and after scattering, one obtains also information on the depth distributions of the different elements with an in-depth resolution of about 20 nm.

The experimental arrangement used for the NRA and RBS measurements [27] consisted basically of a target chamber at high vacuum (about 10^{-7} mbar), which was connected to a beam line of the 7 MeV Van de Graaff Accelerator of the Institut für

Kernphysik. A 5'' × 5'' NaI detector and a silicon surface barrier detector together with standard electronics for pulse-height analysis were used for measuring γ rays and ^4He particles, respectively. Charging of the glass samples was prevented by flooding the surface with electrons from a heated filament. As calibration standard for hydrogen, a silicon crystal implanted with a known fluence of hydrogen ions was used. The calibration for RBS analysis was obtained by comparison with the known concentration values of the components of the SK 16 glass.

Furthermore, a correlation between the optical properties and the results of the in-depth analysis was necessary in order to show the relevance of the analysis data for optical fabrication. Therefore, in addition to measuring the in-depth profiles of the samples, the subsurface layers were characterized by determining their spectral reflectance. This was achieved using the photodiode-array spectrometer in modular design[2]). From the measured spectral reflectance $R(\lambda)$ the refractive index n and the thickness d of the uncoated and coated layers were calculated using a computer program[3]).

2.2. Sample preparation

The main components of the SK 16 glass are: (wt %) $\approx 30\ SiO_2$, $\approx 47\ BaO$ and $\approx 20\ B_2O_3$. The optical surfaces considered in this work were produced at Zeiss by generating, fining and polishing of biconvex photographic lenses in the regular production line. Polytron was used as polishing ground for the cerium oxide polishing slurry. In-depth distributions of the glass components can be obtained within the subsurface layers developed on SK 16 glass by SIMS and IBSCA which have an in-depth resolution of better than 2 nm [3 and 4]. The in-depth resolution of NRA and RBS was about 10 nm (see section 2.1.). In order to recognize concentration changes with NRA and RBS distinctly enough, the thickness of the subsurface layers should be at least an order of magnitude greater than the in-depth resolution of these methods.

It seemed, however, not advantageous to develop much thicker layers because inhomogeneities could be developed by the sputtering process which could decrease the in-depth resolution of the SIMS and IBSCA analysis [34 and 35]. Therefore, a thickness d in the range $100\ nm < d < 200\ nm$ seemed appropiate. The development of such subsurface layers on the polished SK 16 lenses and on polished flat glass surfaces was accomplished by immersion of the samples into polishing slurries with different pH values out of the lens production. The slurry contained, besides other components, the cations of barium, boron and silicon because these were extracted from the subsurface of the glass and the wear particles during polishing. Subsurface layers distinctly thicker than 100 nm could be obtained when a smaller pH value of the slurry was applied for the attack of the glass. It appeared to be convenient to leach the SK 16 glasses considered here with slurries of pH values of 6.2 and 8.5. A value of pH = 8.5 is still close to pH values observed in fabrication lines and therefore the processes disclosed for the subsurface layers developed at pH = 8.5 allow conclusions on processes occuring during fabrication. A duration for the leaching of ≥ 6 h was selected for the present investigations because it was derived from measurements of the spectral reflectance that after this prolonged treatment the final thickness of the subsurface layer was attained.

A part of the SK 16 lenses was coated with a $\lambda/4$-layer of MgF_2 after cleaning the samples in an ultrasonically agitated production machine. The uncoated samples were cleaned by rubbing their surface with alcohol. The coated samples underwent a thermal treatment at 250 °C for 12 h in an N_2 atmosphere. The furnaces used for this treatment were heated with electricity.

3. Results

3.1 Analysis with SIMS and IBSCA

3.1.1. Profiling of coated and uncoated optical surfaces on SK 16 glass

a) Treatment with a slurry of pH = 6.2 for 6 h:

Figure 2a gives the in-depth profiles of $^1H^+$, $^{11}B^+$, $^{24}Mg^+$, $^{28}Si^+$ and $^{138}Ba^+$ ions recorded during continuous sputtering of a coated optical surface and the leached subsurface layer of SK 16 glass, together with the intensity of the emission of the B I line at $\lambda = 249.77$ nm which is characteristic for an excited state of boron sputtered in the neutral state (the in-depth profiles were recorded from the left in figures 2a to e). Figure 2b shows the in-depth profiles for the secondary ions of the very same sample together with the intensity of the emitted Si I line at $\lambda = 288.16$ nm. In the investigations reported here mostly the radiation emitted from the atoms which were sputtered in the neutral state was recorded for a comparison with the secondary ion currents. The MgF_2 coating is shown qualitatively in figures 2a and b on the left by the $^{24}Mg^+$ ion current which shows a steep increase at the surface, a slow increase across the coating and a steep decrease at the interface between the coating and the surface of the glass. The H^+ secondary ion currents recorded during the ion-beam etching of the MgF_2 coating showed that hydrogen was present also within MgF_2. This hy-

[2]) This instrument was developed by Carl Zeiss, Oberkochen (FRG), and is described in various papers which can be ordered from this company.

[3]) Available from Hewlett-Packard, Bad Homburg v. d. H.

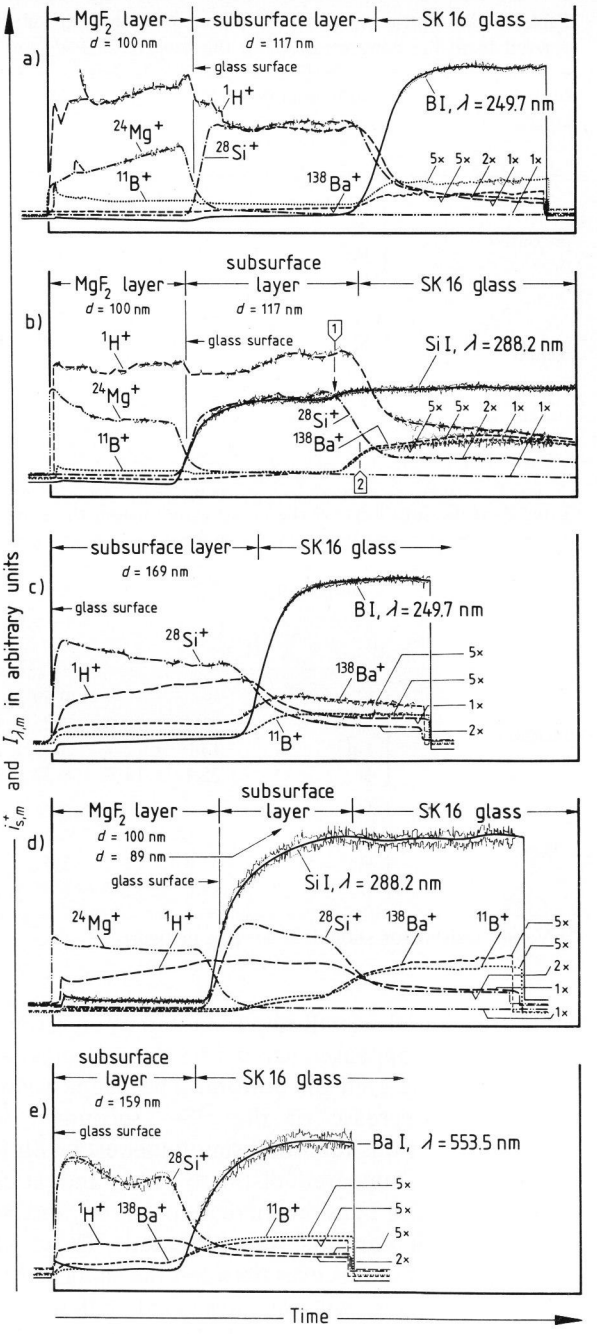

Figures 2a to e. SIMS and IBSCA in-depth profiles of coatings and subsurface layers. 5.6 keV-Ar^+-ion beam was applied with an angle of incidence of $\beta = 60°$; for further details see section 2.1.

The figures 2a to c show in-depth profiles of subsurface layers developed with a slurry of pH = 6.2 after 6 h. For the $\lambda/4$-MgF_2-coated samples the in-depth profiles of the $^1H^+$, $^{11}B^+$, $^{24}Mg^+$, $^{28}Si^+$ and $^{138}Ba^+$ secondary ion currents $i_{s,m}^+$ are given for comparison together with the simultaneously recorded in-depth profiles of the intensities $I_{\lambda,m}$ of the B I emission line with $\lambda = 249.7$ nm and of the Si I emission line at $\lambda = 288.16$ nm in the figures 2a and b, respectively, see section 3.1. and section 4. (part 2). The discharging was done with 170 eV electrons and a Ta diaphragm during the recording of the profiles in figure 2a, whereas 150 eV electrons only were when figure 2b was recorded, when see section 2.1. and the discussion 4.1. and 4.3. in part 2. For an uncoated sample after storage (see text) the in-depth profiles of the $^1H^+$, $^{11}B^+$, $^{28}Si^+$ and $^{138}Ba^+$ secondary ion currents were recorded simultaneously with the in-depth profile of the intensity of the excited B I emission line at $\lambda = 249.77$ nm, figure 2c. For discharging 150 eV electrons only were applied.

The figures 2d and e are in-depth profiles of subsurface layers, which were developed with a slurry of pH = 8.5 after 21 h. For the $\lambda/4$-MgF_2-coated sample, see figure 2d for comparison the in-depth profiles of the same secondary ion currents $i_{s,m}^+$ and the intensity $I_{\lambda,m}$ of the Si I emission line at $\lambda = 288.16$ nm were recorded as for figure 2b. Discharging: 150 eV electrons and Ta diaphragm. For the uncoated sample, figure 2e, the in-depth profiles of the $^1H^+$, $^{11}B^+$, $^{28}Si^+$ and $^{138}Ba^+$ secondary ion currents were recorded simultaneously with the in-depth profile of the intensity of the excited B I emission line at $\lambda = 249.77$ nm (different from the figures 2b and c, there were no shoulders for the $^{11}B^+$ and $^{138}Ba^+$ currents; for discussion, see section 4.3. in part 2). Discharging: 250 eV electrons and Ta diaphragm.

drogen indicates water which could be trapped within MgF_2 layers during coating [36 and 37].

When the ion-beam milling reached the subsurface layer, a decrease of the $^{24}Mg^+$ ion current and simultaneously an increase of the $^{28}Si^+$ ion current was observed. Then the $^{28}Si^+$ and $^1H^+$ secondary ion currents remained almost constant during the removal of the subsurface layer. These shapes show qualitatively greater relative silicon and hydrogen concentrations within the leached layer. A constant $^1H^+$ and $^{28}Si^+$ signal was not observed previously because of the small thickness of the leached layers, which was only of the order of the in-depth resolution of a few nanometers [14 and 19].

The interface between the subsurface layer and the bulk glass is denoted in figures 2a and b by a decrease of the $^1H^+$ and $^{28}Si^+$ secondary ion currents and an increase of the B^+ and Ba^+ currents too. The B^+ and Ba^+ secondary ion currents were distinctly greater than during the sputtering of the subsurface layers and were almost constant during the sputtering of the bulk glass, see also section 4.3. in part 2. The increase of these currents at the interface shows that boron and barium were leached from the subsurface layer. It seems remarkable also, see figure 2a, that the B I intensity showed a higher step than the $^{11}B^+$ secondary ion current.

Distinctly greater $^{28}Si^+$ and $^1H^+$ secondary ion currents are always observed during the ion-beam milling of the subsurface layers other than during the subsequent milling of the bulk glass as described earlier [3 and 4]. As can be seen in figures 2a and b the same phenomenon was observed for the subsurface layers considered here which were formed during a prolonged attack of the polished surface by the slurry (see section 2.). This enhancement of the $^{28}Si^+$ and $^1H^+$ currents allows to detect such subsurface layers developed during polishing [3].

However, the profile of the Si I emission line is quite different from that obtained with SIMS for the Si^+ current (figure 2b). In this figure the intensity of the Si I line was greater during the analysis of the bulk than that of the subsurface layer. The increase of the

Table 1. Concentrations for the components within the subsurface layers developed with a slurry of pH = 6.2 with SIMS and IBSCA, derived from the concentrations of the bulk and SIMS and IBSCA quantities

subsurface layers	components	Q_m^I	Q_m^+	$\frac{(\Delta d/\Delta t)_b}{(\Delta d/\Delta t)_l}$	C_{mb} in $10^{22} \cdot cm^{-3}$	C_{ml} in $10^{22} \cdot cm^{-3}$	
						IBSCA	SIMS
uncoated	H	–	0.22 ± 16 %	0.65	–	–	–
	Si	1.27 ± 10 %	0.21 ± 10 %	0.65	1.11	0.57	3.44
	Ba	10 ± 12 %	3.25 ± 10 %	0.65	0.68	0.044	0.14
	B	19 ± 12 %	5.36 ± 10 %	0.65	1.30	0.045	0.16
coated	H	–	0.18 ± 8 %	1	–	–	–
	Si	1.14 ± 10 %	0.18 ± 10 %	1	1.11	0.98	6.18
	Ba	30 ± 12 %	5.31 ± 7 %	1	0.68	0.023	0.13
	B	26 ± 12 %	3.48 ± 10 %	1	1.30	0.050	0.37

Table 2. Concentrations for the components within the subsurface layers developed with a slurry of pH = 8.5 with SIMS and IBSCA, derived from the concentrations of the bulk and SIMS and IBSCA quantities

subsurface layers	components	Q_m^I	Q_m^+	$\frac{(\Delta d/\Delta t)_b}{(\Delta d/\Delta t)_l}$	C_{mb} in $10^{22} \cdot cm^{-3}$	C_{ml} in $10^{22} \cdot cm^{-3}$	
						IBSCA	SIMS
uncoated	H	–	0.59 ± 8 %	0.72	–	–	–
	Si	1.12 ± 10 %	0.25 ± 13 %	0.72	1.11	0.72	3.20
	Ba	13.0 ± 12 %	3.11 ± 13 %	0.72	0.68	0.018	0.13
	B	25.1 ± 14 %	8.27 ± 10 %	0.72	1.30	0.037	0.11
coated	H	–	0.35 ± 8 %	0.93	–	–	–
	Si	1.08 ± 10 %	0.21 ± 10 %	0.93	1.11	0.96	4.93
	Ba	34.0 ± 12 %	5.02 ± 7 %[4])	0.93	0.68	0.037	0.16
	B	15.5 ± 12 %	3.35 ± 10 %[4])	0.93	1.30	0.078	0.36

[4]) Value derived for shoulders as seen in figure 2d.

intensity formed a small step (denoted by an arrow as point 1) and it appeared just before the bulk glass was reached by the etch pit bottom. The deepest slope during the decrease of the $^{28}Si^+$ secondary ion current, which was recorded simultaneously with the Si I intensity, appeared distinctly later and at the same time (point 2) as the increase of the B^+ and Ba^+ secondary ion currents was observed. These and other apparent differences between the shapes of the in-depth profiles will be discussed below. The in-depth profiles of the uncoated subsurface layers with pH = 6.2 showed almost the same behaviour as the samples with pH = 8.5, (see figures 2c and e). However, the relative increase of the secondary ion currents was different from that of the intensities of the photon-emission lines at the interface for both the uncoated specimens and the coated specimens as well.

b) Treatment with a slurry of pH = 8.5 for 21 h:

Figure 2d gives for comparison in-depth profiles which were recorded for an optical surface which was attacked with a slurry of pH = 8.5 for 21 h before cleaning and coating. In this case the Si I intensity showed no step between the subsurface layer and the bulk, but an almost continuous increase from the interface between the coating and the bulk glass was recorded. Different from what was observed in figures 2a and b, in figure 2d the $^{11}B^+$ and the $^{138}Ba^+$ profiles show a distinct "shoulder" within the subsurface layer. The in-depth profiles recorded for the same specimen before the coating are given in figure 2e. The profiles show that hydrogen, barium and boron are present within this subsurface layer.

c) Comparison of the different in-depth profiles with each other:

Quite a number of in-depth profiles both for coated and uncoated subsurface layers developed with a slurry of pH = 6.2 or pH = 8.5 were recorded. For obtaining an overview over the variations of these numerous in-depth profiles it seemed convenient to characterize the results by the ratios

$$Q_m^+ = i_{mb}^+ / i_{ml}^+$$

of the average ratio of the positive secondary ion currents (l denotes surface layer, b denotes bulk) which were recorded for the component m within the bulk, i_{mb}^+, and within the leached subsurface layer, i_{ml}^+, and by the ratios of the corresponding intensities of the characteristic emission lines

$$Q_m^I = I_{\lambda,mb} / I_{\lambda,ml} .$$

These ratios are given in tables 1 and 2 in the second and third column. In those cases in which "shoulders" were observed during the ablation of the subsurface layers, the greatest values i_m^+ or $I_{m,\lambda}$, respectively, were used for the calculation of the ratios Q. The intensity of the H I line excited at $\lambda = 656.28$ nm was very weak and, furthermore, the in-depth profiles showed a great contribution of the background. Therefore, the concentration of hydrogen was analyzed with NRA, see section 3.3.

It is important to note that the in-depth profiles of the B^+ and Ba^+ secondary ion currents for both pH values are almost constant within the subsurface layers before coating and that no shoulder appeared. Apart from this, however, the same relative increase and decrease of the secondary ion currents and the intensity of the recombination radiation were observed as for the coated specimen.

Special attention has to be paid to peculiarities of the information contained in tables 1 and 2: The ratios Q_m^+ and Q_m^I for the respective elements which were obtained during the removal of the bulk glass and its subsurface layers indicate a removal of barium and boron out of the leached subsurface layers for both pH values. The ratios Q_{Si+} indicate a relatively greater concentration of silicon within the leached layers accordingly, whereas the ratios Q_{Si}^I let suggest a slightly smaller concentration of silicon there.

3.1.2. Comparison of the results for the subsurface layers with those of the bulk

As already mentioned, matrix effects could exist for SIMS [22 and 23] and matrix effects cannot be ruled out for IBSCA as was found for different silica glasses which contain barium and boron [38]. Also calibration standards with a known composition were not available for the subsurface layers considered here.

For a first approximative calculation of the ratios $C_{m\,l}/C_{m\,b}$, it was tentatively assumed that the matrix effects connected with ionization and excitation would be the same for the bulk and the subsurface layers, respectively. Therefore, the quantities $\alpha_{\lambda,m}$ and p_m^+ would not measurably be changed when the interface between the subsurface layer and the bulk was penetrated during sputtering. According to equations (1 and 2) in section 2., in this case both

$$\frac{\alpha_{\lambda,m\,b}}{\alpha_{\lambda,m\,l}} \approx 1 \text{ and } \frac{p_{m\,b}^{\pm}}{p_{m\,l}^{\pm}} \approx 1 .$$

Furthermore, the ratios of the sputter yields $S_{tot\,b}$ and $S_{tot\,l}$ were approximated by the respective rates of the sputtered volumes $(\Delta V/\Delta t)_b$ or $(\Delta V/\Delta t)_l$ for the same sputter conditions.

It has to be mentioned that the sputter yields must be measured in order to obtain an exact comparison of the matrix effects, see also section 4.2. (part 2). The approximation used here holds as long as the volumes ΔV are roughly proportional to the sputter yields S and because in this energy range of the projectile ions the differences in the specific energy losses by non-elastic scattering within the subsurface layers and the bulk can be neglected [39 and 40]. The ion-beam diameter, the ion-beam density and the diameter of the tantalum diaphragms were the same when the rates of the sputtered volumes were measured. Therefore, the ratios $(\Delta V/\Delta t)_b/(\Delta V/\Delta t)_l$ can be replaced by the ratios of the in-depth sputter rates $(\Delta d/\Delta t)_b/(\Delta d/\Delta t)_l$. The latter ratios were derived from plots as given in figure 1, which served for the measurement of the time for reaching the interface between the subsurface layers and the bulk. A method which records the sputter rates continuously is described in [41].

Therefore, the concentrations of the components within the layer were calculated from the known concentrations within the bulk for SIMS using equation (1), section 2.1., with

$$C_{m\,l} = C_{m\,b} \cdot \frac{i_{s,m\,l}}{i_{s,m\,b}} \cdot \frac{(\Delta d/\Delta t)_b}{(\Delta d/\Delta t)_l} \tag{5}$$

and for IBSCA from equation (2), section 2.1., with

$$C_{m\,l} = C_{m\,b} \cdot \frac{I_{\lambda,m\,l}}{I_{\lambda,m\,b}} \cdot \frac{(\Delta d/\Delta t)_b}{(\Delta d/\Delta t)_l} . \tag{6}$$

This comparison implies that the values i, I and $\Delta d/\Delta t$ were measured under the same experimental conditions. For the calculation of the concentration $C_{m\,l}$ the ratios derived from the experiments and listed in the second and third column of tables 1 and 2 can be used, since

$$\frac{i_{s,m\,l}}{i_{s,m\,b}} = \frac{1}{Q_m^+} \text{ and } \frac{I_{\lambda,m\,l}}{I_{\lambda,m\,b}} = \frac{1}{Q_m^I} .$$

In tables 1 and 2 the concentrations of silicon, barium and boron in the bulk are listed together with the quantities $1/Q_m^I$, $1/Q_m^+$, $(\Delta d/\Delta t)_b/(\Delta d/\Delta t)_l$ and the concentrations which were calculated according to equations (5 and 6) for silicon, barium and boron within the subsurface layers.

The ratios Q_m^I obtained for barium and boron were always much greater than the respective values Q_m^+. Thus IBSCA would indicate a smaller concentration of the residual barium and boron within the subsurface layers than SIMS, for both the uncoated and the coated specimen as well (see tables 1 and 2). From the small Q_{Si}^+ values a distinctly greater silicon concentration was calculated for the leached layer whereas from the much larger values Q_{Si}^I the opposite was derived. The ratios of the true sputter yields to be

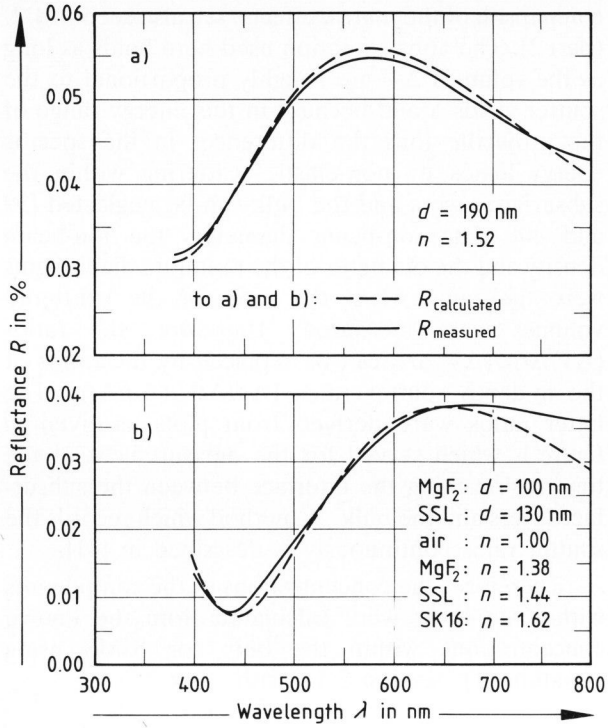

Figures 3a and b. Comparison of the measured and the calculated spectral reflectance of polished optical surfaces on SK 16 glass after the interaction with a slurry of pH = 6.2 for 6 h; a) before coating, b) after coating with a $\lambda/4$-MgF_2 layer.

Table 3. Thickness d of the hydrated subsurface layers from the in-depth calibration by the etch pit depth and from the spectral reflectance, see text in sections 2.1. and 3.2.

	pH = 6.2			pH = 8.5		
	from $R = f(\lambda)$		from etch pits	from $R = f(\lambda)$		from etch pits
	n	d in nm	d in nm	n	d in nm	d in nm
uncoated	1.52 ± 5 %	190 ± 5 %	169 ± 10 %	1.53 ± 5 %	150 ± 5 %	159 ± 10 %
coated	1.44 ± 5 %	130 ± 5 %	117 ± 10 %	1.52 ± 5 %	88 ± 5 %	89 ± 10 %

expected from the differences in the atomic densities can not differ from the ratios of the $\Delta V/\Delta t$ values by more than a factor of two (see also section 4.2., part 2). Therefore, the differences between the exact sputter yields could not account for the differences between the ratios Q_m^{I} and Q_m^{+} and the concentrations listed in tables 1 and 2. Thus in this state of investigations it was obvious that the quantities p_m^{+} and $\alpha_{\lambda,m}$ had changed at the interface. However, it had to be left open which of the two quantities $p_m^{\pm}$ and $\alpha_{\lambda,m}$ in equations (1 and 2), respectively, showed a greater change during the transition of the ion-beam etching from the subsurface layer into the bulk, i. e. produced the greater matrix effect. In order to decide on this question, other surface analysis methods had to be applied, too, which did not depend on the ionized and excited atoms produced during sputtering.

3.2. Thickness and mean refractive index of the uncoated and coated subsurface layers

The spectral reflectance $R = f(\lambda)$ was measured for the coated and uncoated specimens whose in-depth profiles were given in figures 2a to e (see section 3.1.). The spectral reflectance was also modelled under the assumption that changes of the refractive index within the subsurface layers and the coating could be neglected. This approximation seemed justified from the results of the in-depth distribution of the elements and because the deviations of the calculated $R = f(\lambda)$ were within the limits of error which had to be expected for the specimens considered here (see also the discussion given in section 4.3., part 2). In figures 3a and b, e.g., the calculated and the measured spectral reflectances are compared with each other for the uncoated and coated specimens prepared at pH = 6.2 after 6 h. Table 3 gives the mean refractive indices n deduced from the spectral reflectance of the coated and uncoated specimen developed at both pH values, together with the thicknesses of the subsurface layers, which was calculated from the spectral reflectance and those calculated from the shift of the interference fringes caused by the etch pits. The values d deduced from the spectral reflectance generally had a smaller limit of error (about 5 %) and were therefore used with preference for the in-depth calibration.

3.3 Analysis with RBS and NRA

RBS measurements were performed at a MgF_2 coated and an uncoated sample prepared with a slurry of pH = 6.2 and for comparison at an untreated SK 16 glass sample. In figures 4 and 5 the RBS spectra of these samples are displayed. They show clearly the backscattering signals of barium, silicon and oxygen; the boron signal is too weak as to be recognized. The spectrum of the coated sample (curve 1 in figure 4) shows also peaks arising from magnesium and fluorine. The peak at 2.55 MeV (curve 4 in figure 4) is due to a tungsten impurity in the MgF_2 layer introduced during the coating process. The backscattering energies which correspond to the atoms of the different elements at the sample surface are indicated by arrows. The shifts of the oxygen edge and of the silicon edge and a part of the shift of the barium edge in the spectrum of the coated sample to lower energies are due to the MgF_2 layer. The dashed line (curve 3 in figure 4) indicates the shift of the barium edge as it would be observed if the sample was coated without having a leached subsurface layer.

Curve 1 in figure 5 shows that the uncoated sample has a subsurface layer in which the barium

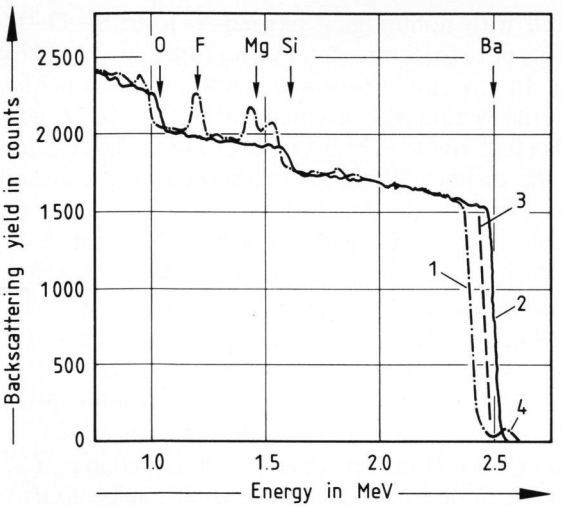

Figure 4. Comparison of the energy distribution of $^4He^+$ ions backscattered from the surface; curve 1: sample leached at pH = 6.2 coated with a $\lambda/4-MgF_2$ layer, Curve 2: sample without a subsurface for reference, curve 3: see text, curve 4: see text.

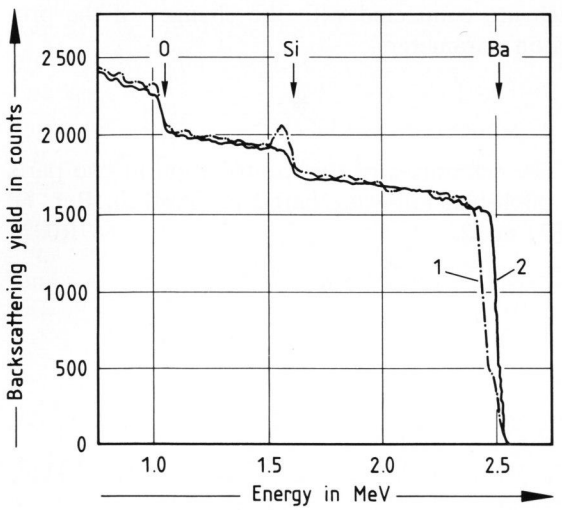

Figure 5. Comparison of the energy distribution of $^4He^+$ ions backscattered from the glass surfaces of an uncoated specimen, leached with a slurry of pH = 6.2, after storage (curve 1) and a sample without a subsurface layer for reference (curve 2).

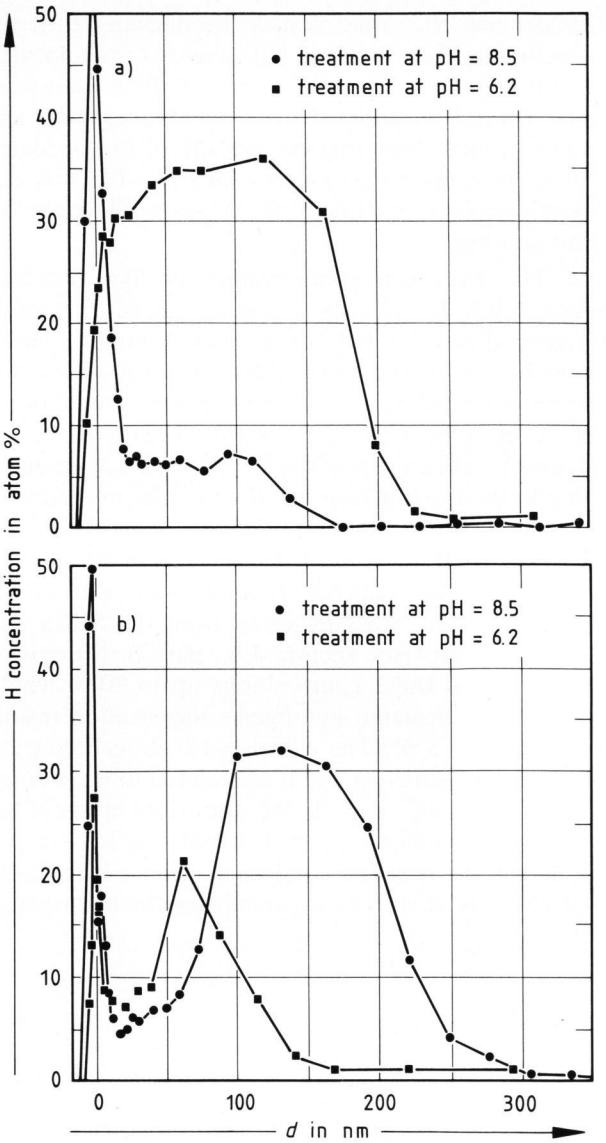

Figures 6a and b. NRA in-depth profiles of hydrogen a) from the uncoated samples treated with slurries of pH = 6.2 and pH = 8.5 for 6 and 21 h; b) from the coated samples treated with slurries of pH = 6.2 and pH = 8.5 for 6 and 21 h before coating.

concentration is reduced compared to the bulk value. The coated sample has a leached layer in which the barium content is almost zero (figure 4). In the spectrum of the coated sample and, to a somewhat lesser extent, in the spectrum of the uncoated sample the backscattering yield below the silicon edge is enhanced relative to the untreated sample, forming broad peaks. This is due to the higher relative silicon concentration in both leached layers compared to the bulk concentration. The SIMS and IBSCA results show that not only barium has been leached out but also boron, in such a way that the ratio C_{Ba}/C_B in the leached layers is the same as in the bulk glass (see section 4.4., part 2). This information was used in the analysis of the RBS spectra. Furthermore, it was assumed that in the subsurface layers barium exists as BaO and boron exists as B_2O_3 (see section 4.4., part 2). From this analysis and using the NRA results on the hydrogen concentration in the subsurface layers (see this section below), the composition of the subsurface layer of the uncoated sample was obtained as $SiO_2 \cdot 0.25\,B_2O_3 \cdot 0.25\,BaO \cdot 0.27\,H_2O$ and that of the coated sample as SiO_2 was obtained with uncertainties of about 20 %; for the coated sample the hydrogen content is rather small (figure 6a). From the widths of the regions with enhanced silicon yield and from the shifts of the barium edge one can deduce the areal densities $d\varrho$ of the leached subsurface layers (d = thickness, ϱ = density). These values are (33 ± 3) µg/cm^2 for the uncoated sample and (30 ± 3) µg/cm^2 for the coated sample. By comparing with the d values calculated from the spectral

reflectance $R(\lambda)$ one obtains the densities ϱ of the leached layers, $\varrho = 1.8 \pm 0.3$ g/cm^3 for the uncoated sample and $\varrho = 2.3 \pm 0.3$ g/cm^3 for the coated sample. Though the limits of error are relatively large and these results show that the density of the uncoated subsurface layer developed with pH = 6.2 was distinctly smaller than that of the subsurface layer below the coating.

The hydrogen concentration profiles obtained with NRA for a coated and an uncoated sample prepared at pH = 6.2 are shown in figures 6a and b together with the corresponding profiles for the samples prepared at pH = 8.5. In the calculation of these profiles from the measured data for γ-ray counts vs. the energy of the $^{15}N^+$ ions, it was assumed that in the leached layers of the samples treated with slurries of pH = 8.5 the reduction of the BaO and B_2O_3 concentrations were the same as in the leached layers of the samples treated with slurries of pH = 6.2. This was suggested from the SIMS and IBSCA results (see section 4.4., part 2). Moreover, variations of these compositions up to 20 % would affect the calculated hydrogen concentration results by less than 5 %. The calculated hydrogen concentrations in figures 6a and b are related to an average "glass molecule"; e. g., in the subsurface layers of the uncoated samples prepared at pH = 6.2 there are 35 H atoms per 65 molecules $SiO_2 \cdot 0.25\,BaO \cdot 0.25\,B_2O_3$. It is to be expected that the hydrogen is linked with nonbridging oxygen to form Si–O–H groups or to form molecular water (see e. g. [26, 29 to 31]). In any case, the stoichiometric formula of the material within the leached subsurface layer was $SiO_2 \cdot 0.25\,BaO \cdot 0.25\,B_2O_3 \cdot 0.27\,H_2O$. The reasons for the distinct difference of the hydrogen concentration within the leached layers of the different samples will be discussed in section 4.4., part 2.

The concentrations analyzed with RBS and NRA within the subsurface layers showed that neither the SIMS nor the IBSCA results given in tables 1 and 2 were correct within the limits of error. Accordingly, SIMS and IBSCA cannot be applied for a quantitative analysis (see also the considerations given in section 3.1.). However, as will be described in part 2, the matrix effects of these two methods can be used to obtain additional information on changes in the atomic arrangement occuring within the subsurface layers during the hydration. Moreover, this information will be most important for the understanding of the changes of the properties of the subsurface layers which are connected with the changes of the production parameters.

*

The references of this contribution in two parts are published following part 2 in Glastech. Ber. **60** (1987) no. 2. 87R0027